

SPECIAL ISSUE ARTICLE

Laser pyrolyzed organosilazane-based Al/ZrO₂ composite coating on stainless steel: Resulting microstructure and mechanical properties

Alexander Horcher¹ | Katja Tangermann-Gerk² | Walter Krenkel¹ |
Michael Schmidt^{2,3,4} | Rajendra K. Bordia⁵  | Günter Motz¹ 

¹ Ceramic Materials Engineering (CME), University of Bayreuth, Bayreuth, Germany

² Bayerisches Laserzentrum GmbH, Erlangen, Germany

³ Institute of Photonic Technologies, Friedrich-Alexander-Universität Erlangen-Nürnberg, Erlangen, Germany

⁴ Erlangen Graduate School in Advanced Optical Technologies (SAOT), Erlangen, Germany

⁵ Department of Materials Science and Engineering, Clemson University, Clemson, South Carolina, USA

Correspondence

Günter Motz, University of Bayreuth, Ceramic Materials Engineering (CME), Prof.-Rüdiger-Bormann-Straße 1, 95447 Bayreuth, Germany.
Email: guenter.motz@uni-bayreuth.de

Funding information

Bundesministerium für Wirtschaft und Energie, Grant/Award Number: ZF4109903AG7; Deutsche Forschungsgemeinschaft, Grant/Award Numbers: 405583003, MO 851/19, SCHM 2115/72

Abstract

Protective ceramic-based coatings are frequently the most suitable solutions for problems like corrosion and wear. It has been shown that the precursor technology is suitable for the preparation of ceramic coatings by pyrolysis in a furnace. However, the required high temperature for the preparation of the ceramic coatings limits this approach to high temperature-resistant substrates. A very innovative approach to overcome this restriction is the use of laser radiation as a thermal source for the pyrolysis of the preceramic polymer. In this paper, we report on a coating system, for steel substrates, consisting of a polysilazane (Durazane 2250) bond coat and a hard and dense top-coat composed of an organosilazane (Durazane 1800) with tetragonal ZrO₂ particles and aluminum flakes as fillers pyrolyzed using Nd:YVO₄ laser. The aluminum fillers led to a significant increase in absorption of the laser energy leading to the formation of a dense coating with a thickness up to 20 μm and a mainly cellular/columnar-dendritic microstructure. The microstructure, mechanical, and tribological behaviors of these composite coatings are reported and compared to those of laser pyrolyzed glass/ZrO₂-filled polysilazane-based coatings reported in the literature.

KEYWORDS

environmental barrier coating, laser pyrolysis, mechanical properties, polymer-derived ceramic

1 | INTRODUCTION

Coatings are the most suitable and cost-effective solutions to improve the surface properties of metals and to protect them against oxidation, corrosion, and wear. As a result, functional coatings improve the performance and lifetime of components. Specifically, ceramic coatings have been developed to improve the resistance against corrosion

and oxidation of metals. Moreover, ceramic coatings are characterized by their high hardness and wear resistance. Established methods to manufacture ceramic coatings are chemical vapor deposition (CVD), physical vapor deposition (PVD), sol-gel process, or thermal spraying. However, in part, the vapor phase processes have some limitations. PVD deposition, for example, involves a complex vacuum process and the deposition rates are comparatively low. Compared to slurry-based processes, this coating method is associated with higher costs. In

Honoring Dr. Mrityunjay Singh

This is an open access article under the terms of the [Creative Commons Attribution](https://creativecommons.org/licenses/by/4.0/) License, which permits use, distribution and reproduction in any medium, provided the original work is properly cited.

© 2021 The Authors. *International Journal of Applied Ceramic Technology* published by Wiley Periodicals LLC on behalf of American Ceramics Society

addition, during CVD and thermal spraying, the substrate is subjected to mechanical and thermal stresses.

An alternative method is the PDC technology (PDC—polymer-derived ceramic).^{1–9} The used precursors are mostly silicon-based polymers like polysiloxane,¹⁰ polysilazane,¹¹ or polycarbosilane.¹² They are converted into an amorphous ceramic by pyrolysis between 500 and 1000°C in a furnace.⁵ The polymers may be applied by conventional coating techniques like dip-, spray-, or spin-coating. The various processing approaches of these polymeric systems and the ability to develop customized material properties are the distinguishing characteristics of the PDC technology.

A drawback is the high shrinkage of the polymer during pyrolysis, which can be higher than 50% by volume.¹³ This is associated with the formation of cracks, pores, and defects due to degassing of organic components and constrained pyrolysis. As a result, only thin ceramic coatings can be made from pure polymers.¹⁴ To overcome this limitation active, passive or meltable fillers can be added. By the specific selection of polymers and fillers, novel ceramic composition with unique properties with respect to chemistry and properties can be realized.

However, the high temperature required to convert the precursors to ceramics limits the use of PDC coatings on high-melting substrate materials, such as superalloys, high-temperature steels, or ceramics, since the substrate is also thermally stressed during pyrolysis of the coating in a furnace. Moreover, the fillers are only embedded in the precursor matrix, leading to a composite coating that has inhomogeneous properties.

A possible solution to overcome these restrictions is the use of laser radiation as energy source for the pyrolysis of preceramic polymers and to melt the fillers in order to obtain a ceramic coating with homogeneous composition, structure, and properties. The focusing ability of the laser beam allows the application of a defined amount of heat into the green-coating, which is limited to the coating without long duration thermal stress on the substrate. Magee et al.¹⁵ and Gonsalves et al.¹⁶ were among the first to demonstrate the crosslinking of a silazane by the interaction between an organosilazane and a laser. Colombo et al.¹⁷ produced thin SiC coatings (70–100 nm) on silicon wafers and SiO₂ substrates by irradiating a polycarbosilane with a pulsed Nd:YAG laser. They also figured out that by adding graphite particles or applying a thin carbon top layer, the absorption of the laser radiation in the polymeric polycarbosilane film can be increased. As a result, ceramic SiC films could be generated without damaging the substrate materials. Krauß¹⁸ investigated the laser pyrolysis behavior of polycarbosilazane coatings on steel and alumina substrates using a Nd:YAG and a CO₂ laser. It was determined that the radiation of the CO₂ laser

is mainly absorbed at the surface of the polysilazane film, so that only the surface was converted to the ceramic. In contrast, using the Nd:YAG laser, volume absorption resulted leading to complete conversion of the coating. Adding fine Al₂O₃-particles further increased the absorption of the laser radiation in the polymer leading to the ability to prepare 5–10 μm thick amorphous Si-C-O-N coatings.

Tangermann et al.¹⁹ generated 20 μm thick polysilazane-based coatings on steel substrates. They used the commercially available polycarbosilazane Durazane 1800 as precursor. To increase the layer thickness, monoclinic ZrO₂ and glass fillers were added to the polysilazane-based coating suspension. The pyrolysis was performed with a Nd:YAG laser. During the laser pyrolysis, the fillers completely melted and a dense uniform coating was formed. A more detailed characterization of the mechanical properties and corrosion behavior of this coating system was carried out by Horcher et al.²⁰ They compared the laser pyrolyzed coatings with furnace pyrolyzed coatings of the same composition. The comparative investigation showed that laser pyrolysis produces significantly denser and crack-free coatings. Due to the absence of pores, these layers also exhibited significantly higher adhesion to the substrate. In pull-off testing, adhesive failure was observed, which indicates a good bonding between the pyrolyzed coating and the substrate. It was also ascertained that the laser pyrolyzed coatings have a higher hardness due to the absence of defects, which was reflected in their significantly improved wear resistance, compared to furnace pyrolyzed coatings. Finally, due to the dense uniform microstructure, the laser pyrolyzed samples showed significantly better corrosion protection properties than the porous furnace pyrolyzed samples.

However, the high glass content of 43 vol.% in the coating reduces the hardness and causes an *inhomogeneous* hardness distribution compared to a predominantly ceramic ZrO₂ coating.¹⁹ To overcome the hardness reducing effect of the glassy phase, in the research reported in this paper, the glass fillers were substituted with aluminum flakes. A coating system composed of a commercial polyorganosilazane, 3 mol% yttria-stabilized zirconia, and aluminum fillers was investigated. ZrO₂ was added as a passive filler to reduce the shrinkage, leading to thicker coatings, and to generate a ceramic-like coating with good mechanical properties. The aluminum fillers were added to increase the absorption of the laser radiation and as low-melting component in order to reduce stresses during solidification of the coating system. This publication includes a comparison of the glass/ZrO₂-filled coatings described by Tangermann et al.¹⁹ and the new Al/ZrO₂-filled composite coatings. The coatings have been characterized and compared with regard to

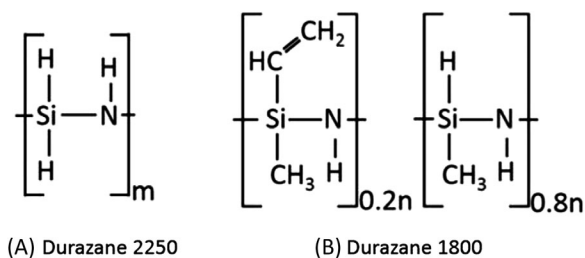


FIGURE 1 Simplified chemical structure of the selected silazanes

their microstructure and mechanical properties, such as hardness, adhesive strength, and abrasion behavior.

This paper reports on a coating system consisting of a polysilazane (Durazane 2250) bond coat and a hard and dense top-coat composed of an organosilazane (Durazane 1800) with tetragonal ZrO_2 particles and aluminum flakes as fillers. The green top-coating was sprayed on the pre-treated steel substrate and subsequently pyrolyzed using Nd:YVO₄ laser. The microstructure of the laser pyrolyzed ceramic coatings was evaluated using scanning electron microscopy (SEM) with energy dispersive X-ray spectroscopy (EDS). Finally, the mechanical properties of the coatings, specifically adhesive strength, hardness, and sliding friction, were investigated.

2 | EXPERIMENTAL PROCEDURE

2.1 | Materials and coating mixture

Two different commercially available polysilazanes, Durazane 2250 (perhydropolysilazane, 20 wt.% in di-n-butylether, previously known as PHPS NN120.20) and the liquid (organo)silazane Durazane 1800, previously known as HTT 1800 (both from Merck KGaA, Germany), were used as precursor materials for the bond-coat and as matrix for the top-coat, respectively. The simplified chemical structure of the polysilazanes used is shown in Figure 1.

In order to improve the crosslinking behavior of Durazane 1800, 3 wt.% DCP (dicumyl peroxide, Sigma-Aldrich Chemie GmbH, Germany) was added to the liquid polymer. Tetragonal ZrO_2 powder (3 mol.% Ytria Stabilized Zirconia, 3YSZ) (ZirPro CY3Z-RS, Saint-Gobain) with a mean particle size $d_{50} = .3 \mu\text{m}$ and a coefficient of thermal expansion (CTE) of $10.5 \times 10^{-6} \text{ K}^{-1}$ was used as passive filler to increase the overall CTE, to reduce the pyrolysis shrinkage, and to improve the surface hardness and wear resistance of the coating. To reduce the melt viscosity and thermal stresses during solidification as well as to improve the absorption of the laser irradiation, aluminum flakes (Alfa Aesar) with an aerodynamic particle size $d_a = 11 \mu\text{m}$ were used.

The preparation of the suspension started with the dissolution of the dispersant DISPERBYK-2150 (BYK-Chemie GmbH, German) in di-n-butylether (purity > 99%, Acros Organics BVBA, Belgium), followed by the addition of the fillers. Finally, the precursor Durazane 1800 was added to the mixture and the suspension was mixed by magnetic stirring. The influence of the precursor content and the fillers on the mechanical properties was investigated. The most promising properties were achieved in a system with 45 vol.% Durazane 1800, 45 vol.% ZrO_2 , and 10 vol.% aluminum flakes, which is described in more detail below.

2.2 | Coating preparation

Flat substrates of 1.5 mm thickness of stainless steel 1.4301, which is a frequently used steel grade in many industrial sectors, were used. The in-plane dimensions of the samples were $75 \times 30 \text{ mm}$. The samples were cleaned in acetone by ultrasonic treatment and dried. Subsequently, a bond-coat of polysilazane Durazane 2250 was applied by dip-coating using a hoisting apparatus (RDC 15, Bungard Elektronik GmbH & Co.KG, Germany) operated with hoisting speed of .5 m/min. The bond-coat was cured in a conventional furnace (N41/H, Nabertherm, Germany) in air at 110°C for 1 h. The resulting layer thickness is about $1 \mu\text{m}$.⁹ The bond-coat prevents the oxidation of the steel substrate during the cross-linking step and pyrolysis and increases the adhesion of the top-coat to the substrate.^{6,7}

The silazane-based coating suspension containing the Al/ ZrO_2 fillers was deposited on the bond-coat by using a spray coater (model 780S-SS Nordson EFD, USA). The spray parameters were adjusted to obtain a green coating thickness of approximately $40 \mu\text{m}$.

Following deposition, the coatings were dried in air at 110°C for 24 h to evaporate the solvent and to crosslink the coating. The crosslinking step stabilizes the green-coating for the laser pyrolysis. The laser pyrolysis was conducted using a Nd:YVO₄ laser ($\lambda = 1064 \text{ nm}$) with a power range up to 10 W (EasyMark 10E, ROFIN-BAASEL Lasertech GmbH Co.KG, Germany) and a focus diameter of the laser beam of about $40 \mu\text{m}$. The laser was operated in a continuous wave (cw) mode. The laser power (P) was varied between 5 and 10 W. The scanning velocity (v) ranged from 6 to 30 mm/s. The laser pyrolysis was conducted in air at room temperature. All experiments were carried out with the coating in focal plane of the laser beam.

2.3 | Coating characterization

The optical absorption behavior of the crosslinked coating was evaluated by UV-VIS-NIR-spectrophotometry (UV-3600, Shimadzu Corporation, Japan) equipped with an

integrating sphere, which allows the measurement of the total and diffuse transmittance and reflectance spectra. The surface and microstructure of the coatings and substrates were examined by light microscope (Axiotech HAL 100, Carl Zeiss Microscopy GmbH, Germany) and SEM (Zeiss Sigma 300 VP, Carl Zeiss AG, Germany). The elemental composition was determined by using an EDS (EDAX Octane Super, EDAX AMETEK GmbH, Germany). The crystalline phases were investigated using X-ray diffraction (Advance D8, Bruker AXS Advanced X-ray Solutions GmbH, Germany). The X-ray diffraction (XRD) pattern of the laser pyrolyzed coating was compared with the furnace pyrolyzed coating in order to determine the influence of the pyrolysis method on the crystalline phases.

The adhesion strength of coatings was evaluated by using pull-off test (ASTM D4541). An aluminum dolly with a diameter of 10 mm was glued onto the surface of the layer. After the adhesive had cured, the assembly was attached to an automatic pull-off tester (PosiTest AT-A, DeFelsko Corp., Ogdensburg, NY, USA). The test device pulls the dolly perpendicular to the plane of the coating and measures the force necessary to detach it from the surface. The applied pulling rate was 1 MPa/s. The microhardness of the coatings was measured by using a hardness tester according to DIN EN ISO 14577 (Fischerscope HM2000, Helmut Fischer GmbH, Germany). A symmetrical pyramidal-shaped diamond indenter is pressed with a force of .098 N into the surface of the sample and the Vickers hardness HV .01 (load 98 mN) is calculated from the mean value of the two diagonals of the indenter. In order to avoid the influence of surface roughness on the results, the measurements were conducted on polished cross-sections. The wear and sliding friction behavior of the coatings was investigated by a testing procedure based on the pin-on-disc method, which enables a fast and efficient realization of friction tests. For the test, hardened and polished steel pins (DIN 1.2367, hardness 580 HV) were used. A surface pressure of 10 MPa and a sliding speed of 10 mm/s have been applied. The tests were conducted at room temperature in linear motions without any coolants or lubricants. The coefficient of friction (COF), which is a dimensionless scalar value and describes the ratio of friction between two bodies, was determined. Before and after the wear tests, the surface roughness of the coatings was evaluated by using a laser-scanning-microscope (LSM, LEXT OLS4000, Olympus Europa SE & Co. KG, Germany).

3 | RESULTS AND DISCUSSION

The laser pyrolysis of the glass/ZrO₂-filled organosilazane-based composite coating has been described in detail by Tangermann et al.¹⁹ In order to define a process window for

the laser pyrolysis of the Al/ZrO₂-composite coating, process parameters, including laser power (p), scanning velocity (v), and distance between adjacent laser tracks (hatching distance h), were systematically varied. The lower range of process window is defined by a parameter combination, which still enables an absorption of laser radiation on the top of green coating. This is a threshold value for the laser energy, above which the interaction of the laser radiation with the green coatings starts. The criterion for an optimum process window was the formation of a homogeneous coating without defects, such as cracks, spalling, or melt agglomerates. In addition, the adhesion of the coating to the substrate was evaluated. Cross-sectional microstructure analysis was used to assess the extent of pyrolysis in the thickness direction.

Green coatings with a thickness of 40–50 μm were successfully pyrolyzed using laser power of 7 W and a scan speed between 10 and 14 mm/s resulting in homogeneous coatings. Compared to the glass/ZrO₂-coatings, the laser power was reduced and the scan velocity was increased. This means that the energy required for layer pyrolysis of the Al/ZrO₂-composite coating is lower than that for the glass-ZrO₂-filled layers and is attributed to the different absorption capacity of the coating systems. Therefore, the reflection and transmission behavior of the Al/ZrO₂-composite coating was measured in order to determine the absorptivity of the coating and compared with the glass containing coating system as described by Tangermann et al.¹⁹ For the 50 μm thick glass/ZrO₂-containing coating, the transmission through the thickness was 31% at 1064 nm—the used wavelength of the laser. The total reflection was measured to be 65%. Hence, Tangermann et al.¹⁹ concluded that the absorption was approximately 4%. Figure 2 shows the reflection and transmission spectrum of the Al/ZrO₂-filled organosilazane-based composite coating.

The reflection and transmission of the Al/ZrO₂-composite coating is shown in Figure 2. The reflection behavior was measured in a wavelength range between 200 and 1800 nm. At the wavelength used ($\lambda = 1064$ nm), the reflection is about 23% (Figure 2A). The peak at 880 nm is a noise signal attributed to the change of the detector during the measurement. The total transmission through the 40 μm thick green Al/ZrO₂-composite coating is almost zero over the entire measuring range (Figure 2B). Accounting for the total reflection of 23%, it may be concluded that the absorption in the coating was 77%, implying that a significantly higher proportion of the laser energy is absorbed in the Al-containing coating compared to the glass/ZrO₂ composite coating. This in turn explains the lower energies required for the pyrolysis of the Al/ZrO₂ composite coating. The significantly increased absorption of laser radiation by this coating system could be mainly

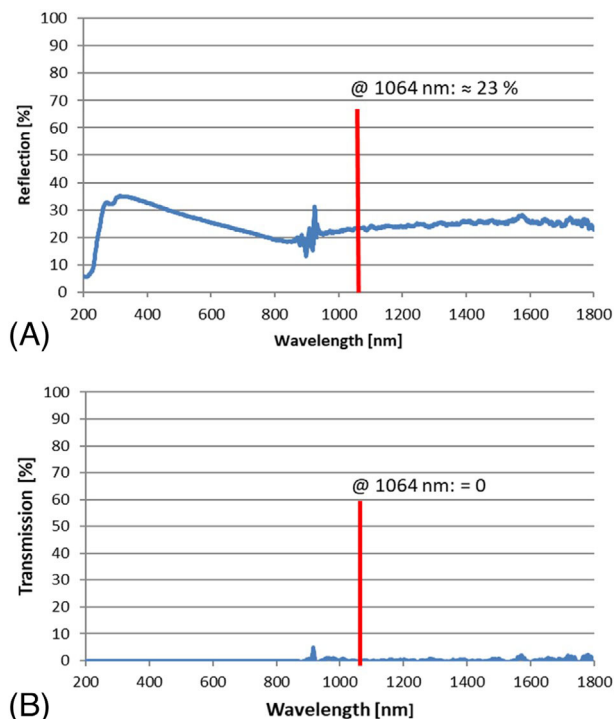


FIGURE 2 UV-VIS-NIR-spectrophotometry of measurements of a 40 μm thick green organosilazane-based coating with 3YSZ and aluminum flakes on a 1 mm thick fused silica substrate: (A): total reflection; (B): total transmission

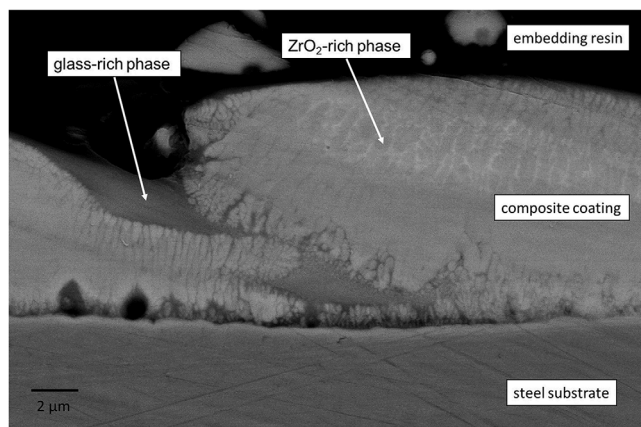


FIGURE 3 Cross-section SEM micrograph of the laser pyrolyzed glass/ZrO₂-filled organosilazane composite coating on stainless steel

attributed to the aluminum flakes. Moreover, the opaque nature of the coating prevents the interaction between the laser radiation and the substrate. Consequently, thermal load on the substrates is significantly reduced.

Tangermann et al.¹⁹ and Horcher et al.²⁰ described the microstructure of the laser pyrolysed glass/ZrO₂ ceramic coating in detail. Results of these investigations are briefly described in the following. Figure 3 shows the SEM image

of the cross-section of the glass/ZrO₂-filled composite coating after laser pyrolysis.

The laser irradiation leads to the generation of dense and crack-free ceramic coatings. The absorption of the laser radiation caused the complete melting of glass fillers, which results in coatings with thicknesses of about 15–20 μm. However, the coating has an inhomogeneous composition with glass- and ZrO₂-rich phases. The silazane is embedded between the molten fillers and homogeneously distributed over the entire coating. The elemental distribution using of this coating system was reported in Ref. 19.

Figure 4 shows SEM images of a laser pyrolyzed Al/ZrO₂-based coating together with the green coating in cross-section. The aluminum flakes are distributed homogeneously in the green coating, embedded in ZrO₂-rich polysilazane-based matrix. The polysilazane acts as a binder between the individual filler particles, resulting in a pore-free green coating after application on the steel substrate. Laser pyrolysis led to densification of the pre-ceramic layers. The coating is dense, however; vertical cracks are present which are attributed to thermal stresses during the rapid cooling stage. The micrographs show the compaction of the green coating as a result of the laser pyrolysis. Ceramic coatings with a thickness of 15–20 μm resulted from laser pyrolysis of 40 μm green coatings, which means a contraction of more than 50%.

High-resolution SEM images in Figure 5 show the microstructure of the laser pyrolyzed coating.

The complete melting of the Al/ZrO₂ composite coating and the rapid solidification of the melt is confirmed by the formation of a predominantly dendritic structure (Figure 5D). However, a fine-grained uniform structure has formed in the vicinity of the steel substrate due to the higher thermal conductivity of the stainless steel substrate compared to the coating, which leads to high temperature gradients and solidification rates within the coating close to the substrate.^{21,22} With increasing distance from the substrate, the heat is increasingly dissipated into the adjacent colder coating areas. This leads to a reduction of the temperature gradient and the cooling rate, resulting in a transition to a cellular/columnar-dendritic solidification structure, as shown in Figure 5B–D.^{21–23} To evaluate the element distribution as well as the chemical composition of the coating, element mappings were carried out using EDS. Figure 6 shows the examined area of the coating and the corresponding EDS mappings.

The main components of the coatings are silicon (Si), zirconium (Zr), oxygen (O), and aluminum (Al). The main components of the stainless steel substrate are iron and the alloying element chromium.

The surface of the coating shows an enrichment of oxygen, silicon, and to some extent of aluminum. Silicon can be assigned to the polysilazane. The enrichment of

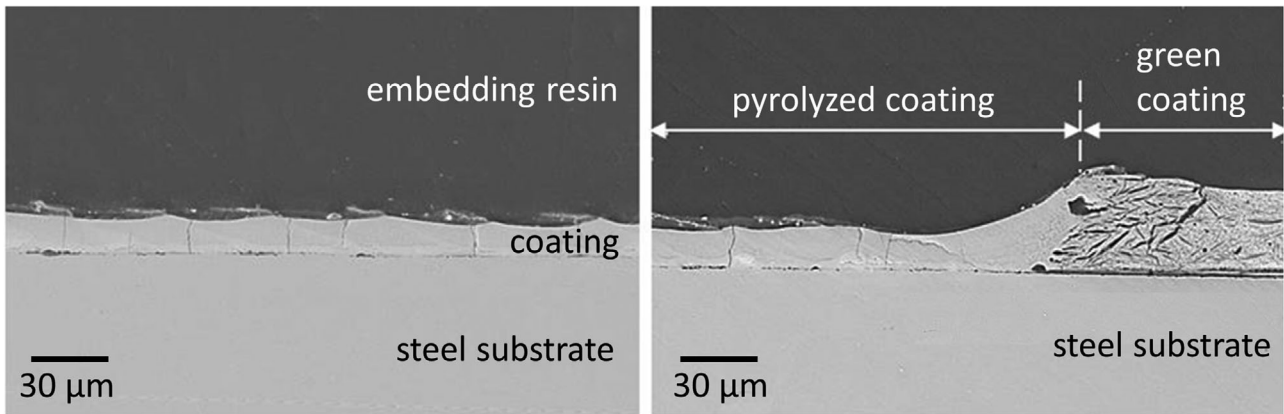


FIGURE 4 Cross-section SEM micrographs of the Al/ZrO₂-filled organosilazane-based coating on stainless steel, with green coating (single irradiation, SE mode), $P = 7 \text{ W}$, $v = 14 \text{ mm/s}$, and $h = 50 \text{ μm}$

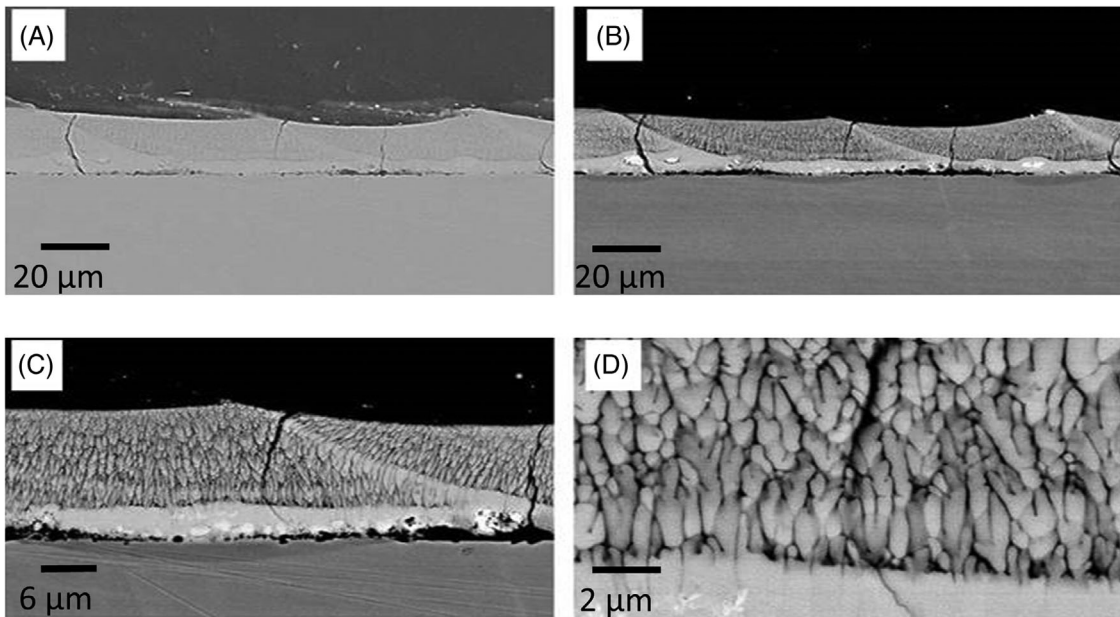


FIGURE 5 SEM images of the pyrolyzed coating on stainless steel, showing details of the microstructure (A: SE mode, B–D: BSE mode)

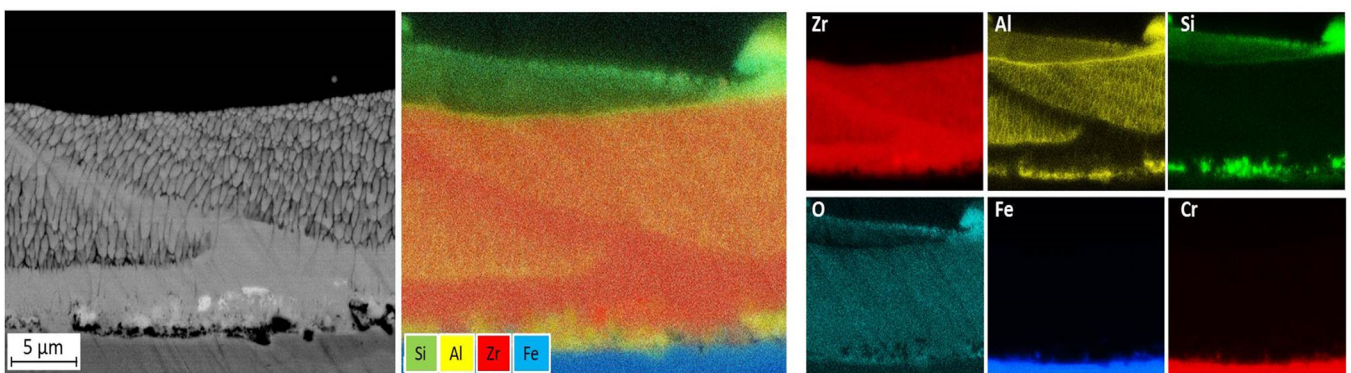


FIGURE 6 SEM image with EDS mapping of the elements of the coating after laser pyrolysis

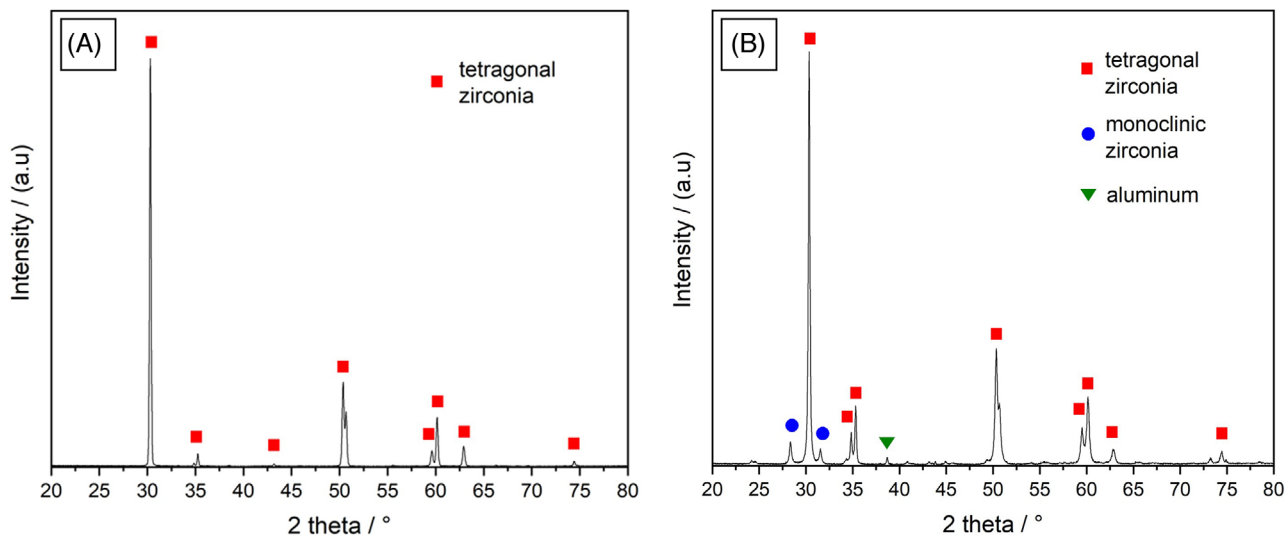


FIGURE 7 X-ray diffraction spectrum of the resulting coating after (A) laser pyrolysis and (B) furnace pyrolysis

aluminum and silicon on the surface is due to the evaporation and recondensation of components of the polysilazane and aluminum.¹⁸ However, this precipitation could be removed with a cloth, which indicates a weak adhesion to the underlying coating. A similar observation was made by Horcher et al.²⁰ during laser pyrolysis of a polysilazane-based glass/ZrO₂ coating on a steel substrate. The underlying compact coating itself consists primarily of a zirconium-rich phase. Enrichments of the elements Al and O were detected at the grain boundaries of the ZrO₂ dendrites. Thus, the coating exhibits a much more homogeneous element distribution than the glass-ZrO₂-composite coating, which in turn has a positive effect on the resulting properties of the coating.

Since surface hardness influences the abrasion resistance of coatings, microhardness of the glass- and Al-containing coating was determined. The average hardness of the laser pyrolyzed glass/ZrO₂ and Al/ZrO₂ coatings is 12.98 ± 1.61 GPa and $21.19 \pm .9$ GPa, respectively. The hardness of Al/ZrO₂ coatings is almost a factor of 2 higher than that of the glass/ZrO₂-filled organosilazane composite coating. The high surface hardness of the laser pyrolyzed Al/ZrO₂-filled composite coating results from the dense and almost complete ceramic microstructure as well as of the homogeneous composition over the entire coating. In addition, a fine-grained structure in the nano-micrometer range also contributed to the high hardness of ceramic materials.²⁴ In comparison, conventionally processed ZrO₂-based ceramics have a hardness of approx. 12–14 GPa.²⁵ Amorphous SiCN-based hard coatings, on the other hand, which are applied by PVD and CVD processes, have a hardness of 20 GPa²⁶ and 12–19 GPa,²⁷ respectively. Thus, the hardness of the laser pyrolyzed coatings is in the order of magnitude of the aforementioned hard coatings.

The presence of the crystalline phases within the coatings was investigated by XRD (Figure 7). Only tetragonal ZrO₂ was detected as the crystalline phase (Figure 7A), which differs from the results obtained in furnace pyrolysis where monoclinic ZrO₂ was also detected (Figure 7B). The furnace pyrolyzed sample was prepared at a temperature of 700°C and a holding time of 1 h. Furthermore, aluminum was detected, which can be attributed to the Al fillers. In the laser pyrolyzed coatings, no aluminum or Al₂O₃ could be detected. Based on this and taking into account the EDS mappings, it is considered that an amorphous Al-, Si-, and O-containing phase has been generated between the dendrites. The stabilization of the high-temperature tetragonal modification of ZrO₂ in laser pyrolysis is probably due to the incorporation of Al₂O₃ from the amorphous phase into the crystal structure of ZrO₂. The stabilizing effect of Al₂O₃ for the tetragonal ZrO₂ modification has been reported in the literature.²⁸ This transformation is a diffusionless displacive phase transformation, which occurs very quickly. The stabilization of the tetragonal modification is an important requirement for the use of ZrO₂ ceramics since the transformation is associated with a volume expansion of 5–8% leading to the formation of cracks. The stabilization of the tetragonal phase has also the advantage of improving the mechanical properties, such as flexural strength, of the ZrO₂ ceramic. The same results were obtained in the glass/ZrO₂-filled polysilazane-based coating system, where the glass constituents stabilized the tetragonal phase.¹⁹

For improved abrasion resistance, the ceramic coating should significantly increase the surface hardness compared to the uncoated steel substrate. Another requirement is good adhesion between the substrate and the coating. Adhesion tests were conducted on these

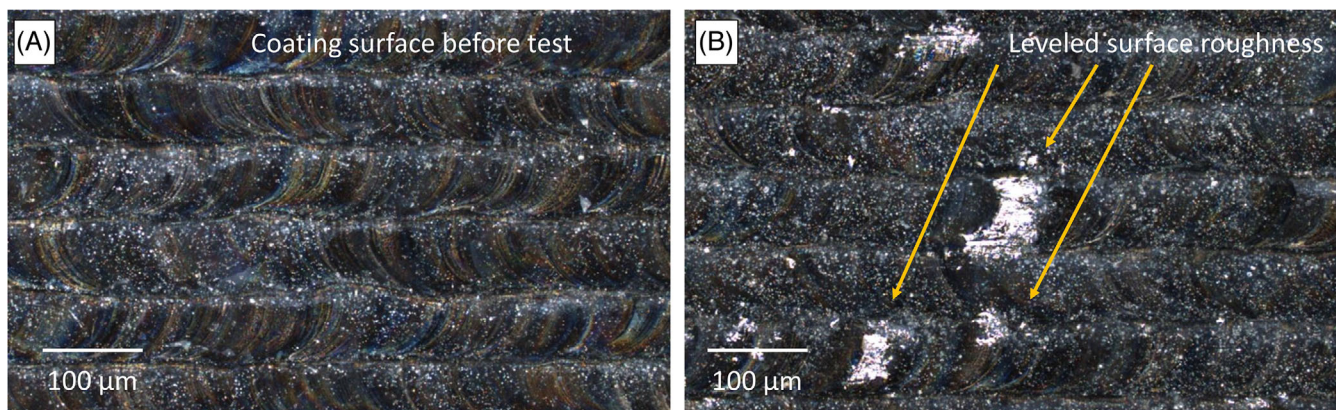


FIGURE 8 Microscopy image of the double-irradiated surface of the Al/ZrO₂-filled polysilazane-based coating (A) before and (B) after tribological test, surface pressure: 10 MPa, feed rate: 10 mm/s

coatings. The average pull-off adhesion strength of the laser pyrolyzed Al/ZrO₂-filled organosilazane-based coatings was 32.7 MPa ($n = 5$, SD = 1.6 MPa). The average pull-off adhesion of the glass/ZrO₂-filled composite coating was 23.8 MPa.²⁰ The higher adhesive strength of the aluminum-filled layer can be attributed to the homogeneous and coating structure. Additionally, the partial wettability of zirconia by molten aluminum leads to chemical bonding of the individual dendrites, resulting in the formation of a compact and dense coating with high cohesion strength.²⁹

In both coating systems, primarily adhesive failure was observed, which indicates a good bonding between the bond-coat and the top-coat and within the top-coat. Horcher et al.²⁰ concluded that there are mainly two reasons for this strong adhesion of the laser pyrolyzed polysilazane-based composite coating. First, the interface between the coating and substrate is free of cracks and pores as shown in Figures 3–5. It is known that a defect above a critical size can induce a macroscopic crack under tensile load, which in turn leads to a reduction of adhesive strength.³⁰ Second, the silazane forms direct chemical bonds with the metallic substrate and fillers, which improves the adhesion.^{9,31} According to the investigations of Amouzou et al.,³² direct chemical bonds are formed between silazanes and stainless steel substrates.

One important attribute of ceramic coatings is their ability to improve wear resistance. However, the wear resistance of coatings depends on many factors, including hardness, coating morphology, fracture toughness, adhesion of the coating to the substrate, and surface roughness.^{30,33,34} In addition, the COF is an important quantity in the development of wear-resistant coatings and should be kept as low as possible to avoid sliding wear.

The COF for sliding friction (dry) between the coating and a steel pin (1.2367, hardness 580 HV) was determined by pin-on-disc tests. In the test procedure, the steel pin is

moved over the surface with a surface pressure of 10 MPa and a feed rate of 10 mm/s. The length of the wear track is 10 mm. The images taken on the laser scanning microscope (LSM) show that abrasive wear is taking place (Figure 8). In order to investigate the effect of the surface roughness on the abrasion behavior, the mean roughness depth R_z of the coating surface before and after testing was measured by using LSM. The mean roughness depth of the coating was $5.39 \pm .53 \mu\text{m}$, which was reduced to $4.35 \pm .39 \mu\text{m}$ after testing. However, no cracking, delamination, or spalling was detected. The good adhesion of the coating to the substrate is of crucial importance in preventing spalling of the coating since contact stresses are transmitted to the substrate and sliding motion results in shear stresses at the interface. For good wear resistance, the interface bonding should be strong enough to withstand these shear stresses without spallation.³⁰ Furthermore, it has been concluded that the abrasive removal as a consequence of the penetration of the steel pin into the coating can be excluded, since the steel pin has a lower hardness compared to the pyrolyzed polysilazane-based coatings.²⁰

In general, the laser pyrolyzed coating is characterized by a large number of small roughness peaks and a wave-shaped contour (Figure 8). This is related to the linear scanning movement of laser beam during pyrolysis, since molten coating materials overlap the preceding pyrolyzed material. During the wear test, these roughness peaks are leveled by the applied pressure and resulting shear forces.²⁰ The leveling effect is evident in the reduction of roughness, which is attributed to an abrasive wear of the peaks. Roughness peaks provoke frictional resistance and interlocking of the surface during the contact of the steel pin and the coating, which influence the COF.²⁰ For the Al/ZrO₂ organosilazane-based coating, a COF $.22 \pm .01$ was determined.

In contrast, the COF for glass/ZrO₂-filled organosilazane-based coating was .33. The surface

roughness of the glass-containing coatings is below the Al/ZrO₂-filled composite coatings. The respective roughness values of the glass-containing coatings before and after testing as well as after single and double irradiation are described by Horcher et al.²⁰ Despite a higher surface roughness, the COF values of the Al/ZrO₂-filled coatings are lower than that of the glass/ZrO₂-filled coatings. This is attributed to the higher surface hardness, and the uniform morphology and phase composition.

The COF of the coatings are in a similar range as those for other ceramic coatings on steel. For example, for ceramic coatings of different composition, the COF values were determined to be: .4–.5 for Al₂O₃, .3–.5 for SiC, .5–.6 for Si₃N₄, and .3–.5 for ZrO₂.³⁵ However, it must be emphasized that the COF is a system parameter and depends on many material and measuring condition factors, including, for example, the material couple, surface quality, applied load, temperature, and humidity.

4 | CONCLUSION

In this work, the laser pyrolysis and characteristics of an organosilazane-based Al/ZrO₂ composite coating system were investigated and their microstructure and mechanical properties compared with a laser pyrolyzed glass/ZrO₂-filled organosilazane-based composite coating. The results show that, despite the short interaction time, the absorption of the Nd:YVO₄ laser radiation ($\lambda = 1064$ nm) within the green coatings was sufficient to obtain dense ceramic composite coatings. By adding aluminum as a filler, the absorption could be significantly increased and transmission reduced compared to glass/ZrO₂-filled coatings enabling the pyrolysis of the coating at lower laser power. In addition, the conversion is uniform through the thickness resulting in dense uniform microstructure.

However, the coatings show stress-induced vertical cracks. The interaction of the laser radiation with the coating leads to complete melting of the aluminum and ZrO₂ fillers. During solidification, a predominate cellular/columnar-dendritic microstructure was formed. The maximum coating thickness was 20 μ m.


The mechanical properties of laser pyrolyzed Al/ZrO₂ composite coatings are promising and better than the glass/ZrO₂ filled coating. The hardness of the glass/ZrO₂-filled polysilazane-based coating was 12.98 GPa and exhibited an adhesive strength of 23.8 MPa. With the Al/ZrO₂-filled coating system, both hardness and adhesion strength were significantly increased—average hardness of 21.19 GPa and adhesive strength of 35.4 MPa. In addition, the laser pyrolyzed coatings protect the substrate effectively against wear and show a low COF of .22.

In summary, laser pyrolysis of the investigated system has great potential for processing of environmental barrier coatings and wear-resistant coatings. Due to selective pyrolysis and short duration under laser beam, this approach has potential for applying ceramic coatings on substrates with limited thermal stability like steel or lower-melting light metals.

ACKNOWLEDGMENTS

The authors would like to thank DFG (Deutsche Forschungsgemeinschaft) for the financial support within the projects 405583003 (MO 851/19 and SCHM 2115/72) and by the Federal Ministry of Germany for Economic Affairs and Energy (BMWi) in the frame of the ZIM cooperation program project number ZF4109903AG7.

ORCID

Rajendra K. Bordia  <https://orcid.org/0000-0001-9256-0301>

Günter Motz  <https://orcid.org/0000-0002-8010-068X>

REFERENCES

- Barroso G, Kraus T, Degenhardt U, Scheffler M, Motz G. Functional coatings based on preceramic polymers. *Adv Eng Mater.* 2016;18(5):746–53.
- Barroso GS, Krenkel W, Motz G. Low thermal conductivity coating system for application up to 1000°C by simple PDC processing with active and passive fillers. *J Eur Ceram Soc.* 2015;35(12):3339–48.
- Wang K, Unger J, Torrey JD, Flinn BD, Bordia RK. Corrosion resistant polymer derived ceramic composite environmental barrier coatings. *J Eur Ceram Soc.* 2014;34(15):3597–606.
- Wang YM, Tian H, Quan DL, Guo LX, Ouyang JH, Zhou Y, et al. Preparation, characterization and infrared emissivity properties of polymer derived coating formed on 304 steel. *Surf Coat Technol.* 2012;206(18):3772–6.
- Günthner M, Wang K, Bordia RK, Motz G. Conversion behaviour and resulting mechanical properties of polysilazane-based coatings. *J Eur Ceram Soc.* 2012;32(9):1883–92.
- Wang K, Günthner M, Motz G, Bordia RK. High performance environmental barrier coatings, Part II: active filler loaded SiOC system for superalloys. *J Eur Ceram Soc.* 2011;31(15):3011–20.
- Günthner M, Schütz A, Glatzel U, Wang K, Bordia RK, Greißl O, et al. High performance environmental barrier coatings, Part I: passive filler loaded SiCN system for steel. *J Eur Ceram Soc.* 2011;31(15):3003–10.
- Kappa M, Kebianyor A, Scheffler M. A two-component preceramic polymer system for structured coatings on metals. *Thin Solid Films.* 2010;519(1):301–5.
- Günthner M, Kraus T, Dierdorf A, Decker D, Krenkel W, Motz G. Advanced coatings on the basis of Si(C)N precursors for protection of steel against oxidation. *J Eur Ceram Soc.* 2009;29(10):2061–8.
- Torrey JD, Bordia RK. Processing of polymer-derived ceramic composite coatings on steel. *J Am Ceram Soc.* 2008;91(1):41–5.
- Lukacs A. Polysilazane precursor to advanced ceramics. *Am Ceram Soc Bull.* 2007;86:9301–6.

12. Colombo P, Paulson T, Pantano C. Synthesis of silicon carbide thin films with polycarbosilanes (PCS). *J Am Ceram Soc.* 1997;80:2333–40.
13. Greil P. Active-filler-controlled pyrolysis of preceramic polymers. *J Am Ceram Soc.* 1995;78(4):835–48.
14. Barroso G, Li Q, Bordia RK, Motz G. Polymeric and ceramic silicon-based coatings—a review. *J Mater Chem A.* 2019;7(5):1936–63.
15. Magee AP, Strutt PR, Gonsalves KE. Laser-induced conversion of molecular precursors to thin films and deposited layers. *Chem Mater.* 1990;2(3):232–5.
16. Gonsalves KE, Strutt PR, Xiao TD, Klemens PG. Synthesis of Si(C,N) nanoparticles by rapid laser polycondensation/crosslinking reactions of an organosilazane precursor. *J Mater Sci.* 1992;27:3231–8.
17. Colombo P, Martucci A, Fogato O, Villoresi P. Silicon carbide films by laser pyrolysis of polycarbosilane. *J Am Ceram Soc.* 2001;84(1):224–6.
18. Krauß HJ. *Laserstrahlinduzierte Pyrolyse präkeramischer Polymere; (Laser-induced pyrolysis of preceramic polymers)*. Bamberg: Meisenbach; 2007.
19. Tangermann-Gerk K, Barroso G, Weisenseel B, Greil P, Fey T, Schmidt M, et al. Laser pyrolysis of an organosilazane-based glass/ZrO₂ composite coating system. *Mater Des.* 2016;109:644–51.
20. Horcher A, Tangermann-Gerk K, Barroso G, Schmidt M, Motz G. Laser and furnace pyrolyzed organosilazane-based glass/ZrO₂ composite coating system—a comparison. *J Eur Ceram Soc.* 2020;40(7):2642–51.
21. Poprawe R. *Lasertechnik für die Fertigung; (Laser technology for manufacturing)*. Berlin Heidelberg: Springer-Verlag; 2005.
22. Kurz W, Fisher DJ. *Fundamentals of solidification*. Trans Tech Publication Ltd; 1992.
23. DebRoy T, Wei HL, Zuback JS, Mukherjee T, Elmer JW, Milewski JO, et al. Additive manufacturing of metallic components – process, structure and properties. *Prog Mater Sci.* 2018;92:112–224.
24. Vasylykiv O., Sakka Y, Skorokhod VV. Hardness and fracture toughness of alumina-doped tetragonal zirconia with different yttria contents. *Mater Trans.* 2003;44(10):2235–8.
25. Elias CN, dos Santos HES, Garbossa M, dos Santos C. Mechanical properties of zirconia Y-TZP core veneered for dentistry applications. *J Ceram Sci Technol.* 2017;8(4):525–30.
26. Allebrandt (Probst) D, Hoche H, Scheerer H, Broszeit E, Berger C. Oxidation resistance of SiAlCN: H-coatings. *Surf Coat Technol.* 2007;201:5172–5.
27. Probst D, Hoche H, Zhou Y, Hauser R, Stelzner T, Scheerer H, et al. Development of PE-CVD Si/C/N:H films for tribological and corrosive complex-load conditions. *Surf Coat Technol.* 2005;200:355–9.
28. Tsubakino H, Sonoda K, Nozato R. Martensite transformation behavior during isothermal ageing in partially stabilized zirconia with and without alumina addition. *J Mater Sci Lett.* 1993;12:196–98.
29. Subramanian P, Zong G, Marcus HL. Selective laser sintering and reaction sintering of ceramic composites. *Proceedings of SFF Symposium.* 1992;63–71
30. Page TF, Knight JC. Factors affecting the tribological behavior of thin hard TiN and TiC coatings. *Surf Coat Technol.* 1989;39–40:339–54.
31. Barroso G. *Thermal barrier coating by polymer-derived ceramic technique for application in exhaust systems*. Göttingen: Cuvillier Verlag; 2018.
32. Amouzou D, Fourdrinier L, Maseri F, Sporcken R. Formation of Me-O-Si covalent bonds at the interface between polysilazane and stainless steel. *Appl Surf Sci.* 2014;320:519–23.
33. Wu L, Guo X, Zhang J. Abrasive resistant coatings—a review. *Lubricants.* 2014;2:66–89.
34. Kennedy DM, Hashmi MSJ. Methods of wear testing for advanced surface coatings and bulk materials. *J Mater Process Technol.* 1998;77:246–53.
35. Klaffke D. Influence of counter body material and relative humidity on the tribological behavior of steel/ceramic couples. *Proceedings, 2nd World Tribology Congress, Vienna, Austria; 2001.*

How to cite this article: Horcher A, Tangermann-Gerk K, Krenkel W, Schmidt M, Bordia RK, Motz G. Laser pyrolyzed organosilazane-based Al/ZrO₂ composite coating on stainless steel: Resulting microstructure and mechanical properties. *Int J Appl Ceram Technol.* 2022;19:856–865. <https://doi.org/10.1111/ijac.13917>